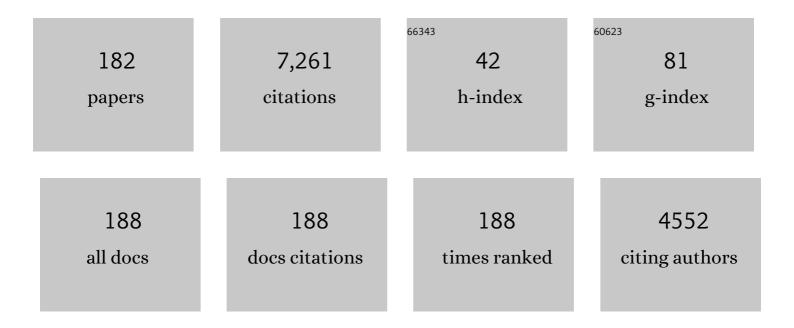
## Robert A Dekemp

List of Publications by Year in descending order

Source: https://exaly.com/author-pdf/1981748/publications.pdf Version: 2024-02-01



#	Article	IF	CITATIONS
1	Data-driven motion correction rescues interpretation of rubidium PET scan with extreme breathing artifacts. Journal of Nuclear Cardiology, 2023, 30, 818-822.	2.1	1
2	Diagnosis of unrecognized aortic dissection by hybrid PET/CT rubidium-82 imaging. Journal of Nuclear Cardiology, 2023, 30, 848-850.	2.1	0
3	Prognostic utility of longitudinal quantification of PET myocardial blood flow early post heart transplantation. Journal of Nuclear Cardiology, 2022, 29, 712-723.	2.1	12
4	Evolving use of PET viability imaging. Journal of Nuclear Cardiology, 2022, 29, 1000-1002.	2.1	2
5	Does quantification of [11C]meta-hydroxyephedrine and [13N]ammonia kinetics improve risk stratification in ischemic cardiomyopathy. Journal of Nuclear Cardiology, 2022, 29, 413-425.	2.1	1
6	One-tissue compartment model for myocardial perfusion quantification with N-13 ammonia PET provides matching results: A cross-comparison between Carimas, FlowQuant, and PMOD. Journal of Nuclear Cardiology, 2022, 29, 2543-2550.	2.1	5
7	Anti-inflammatory effect of rosuvastatin in patients with HIV infection: An FDG-PET pilot study. Journal of Nuclear Cardiology, 2022, 29, 3057-3068.	2.1	7
8	Metabolic activity of the left and right atria are differentially altered in patients with atrial fibrillation and LV dysfunction. Journal of Nuclear Cardiology, 2022, 29, 2824-2836.	2.1	2
9	Static CT myocardial perfusion imaging: image quality, artifacts including distribution and diagnostic performance compared to 82Rb PET. European Journal of Hybrid Imaging, 2022, 6, 1.	1.5	1
10	Myocardial perfusion quantification with Rb-82 PET: good interobserver agreement of Carimas software on global, regional, and segmental levels. Annals of Nuclear Medicine, 2022, 36, 507-514.	2.2	2
11	Evaluation of Lung Glucose Uptake with Fluorine-18 Fluorodeoxyglucose Positron Emission Tomography/CT in Patients with Pulmonary Arterial Hypertension and Pulmonary Hypertension Due to Left Heart Disease. Annals of Nuclear Cardiology, 2022, , .	0.2	0
12	More evidence for adequate test–retest repeatability of myocardial blood flow quantification with 82Rb PET/CT. Journal of Nuclear Cardiology, 2021, 28, 2872-2875.	2.1	0
13	Increased myocardial oxygen consumption rates are associated with maladaptive right ventricular remodeling and decreased event-free survival in heart failure patients. Journal of Nuclear Cardiology, 2021, 28, 2784-2795.	2.1	8
14	Site qualification and clinical interpretation standards for 99mTc-SPECT perfusion imaging in a multi-center study of MITNEC (Medical Imaging Trials Network of Canada). Journal of Nuclear Cardiology, 2021, 28, 2712-2725.	2.1	1
15	Reproducible Quantification of Regional Sympathetic Denervation with [11C]meta-Hydroxyephedrine PET Imaging. Journal of Nuclear Cardiology, 2021, 28, 2745-2757.	2.1	5
16	Validation of multiparametric rubidium-82 PET myocardial blood flow quantification for cardiac allograft vasculopathy surveillance. Journal of Nuclear Cardiology, 2021, 28, 2286-2298.	2.1	12
17	Comparison of myocardial blood flow and flow reserve with dobutamine and dipyridamole stress using rubidium-82 positron emission tomography. Journal of Nuclear Cardiology, 2021, 28, 34-45.	2.1	7
18	Internal validation of myocardial flow reserve PET imaging using stress/rest myocardial activity ratios with Rb-82 and N-13-ammonia. Journal of Nuclear Cardiology, 2021, 28, 835-850.	2.1	6

#	Article	IF	CITATIONS
19	On the roles of reproducibility, ethics, and statistical modeling in medical research. Journal of Nuclear Cardiology, 2021, 28, 855-858.	2.1	2
20	Response to Poitrasson-Rivière and Murthy. Journal of Nuclear Cardiology, 2021, 28, 863.	2.1	3
21	Positron Emission Tomography Imaging of Regional Versus Global Myocardial Sympathetic Activity to Improve Risk Stratification in Patients With Ischemic Cardiomyopathy. Circulation: Cardiovascular Imaging, 2021, 14, e012549.	2.6	6
22	Persistent Lung Inflammation After Clinical Resolution of Community-Acquired Pneumonia as Measured by 18FDG-PET/CT Imaging. Chest, 2021, 160, 446-453.	0.8	9
23	[11C]meta-hydroxyephedrine PET evaluation in experimental pulmonary arterial hypertension: Effects of carvedilol of right ventricular sympathetic function. Journal of Nuclear Cardiology, 2021, 28, 407-422.	2.1	1
24	Regional Distribution of Fluorine-18-Flubrobenguane and Carbon-11-Hydroxyephedrine for Cardiac PET Imaging of Sympathetic Innervation. JACC: Cardiovascular Imaging, 2021, 14, 1425-1436.	5.3	16
25	Quantitative blood flow evaluation of vasodilation-stress compared with dobutamine-stress in patients with end-stage liver disease using 82Rb PET/CT. Journal of Nuclear Cardiology, 2020, 27, 2048-2059.	2.1	12
26	Differential association of diabetes mellitus and female sex with impaired myocardial flow reserve across the spectrum of epicardial coronary disease. European Heart Journal Cardiovascular Imaging, 2020, 21, 576-584.	1.2	8
27	Nuclear Imaging of the Cardiac Sympathetic Nervous System. JACC: Cardiovascular Imaging, 2020, 13, 1036-1054.	5.3	40
28	Reliable quantification of myocardial sympathetic innervation and regional denervation using [11C]meta-hydroxyephedrine PET. European Journal of Nuclear Medicine and Molecular Imaging, 2020, 47, 1722-1735.	6.4	7
29	Effect of proton pump inhibitors on Rubidium-82 gastric uptake using positron emission tomography myocardial perfusion imaging. Journal of Nuclear Cardiology, 2020, 27, 1443-1451.	2.1	5
30	Validation of regional myocardial blood flow quantification using three-dimensional PET with rubidium-82: repeatability and comparison with two-dimensional PET data acquisition. Nuclear Medicine Communications, 2020, 41, 768-775.	1.1	1
31	Exploring Occupational, Recreational, and Environmental Associations in Patients With Clinically Manifest Cardiac Sarcoidosis. CJC Open, 2020, 2, 585-591.	1.5	4
32	Atrial Arrhythmias in Clinically Manifest Cardiac Sarcoidosis: Incidence, Burden, Predictors, and Outcomes. Journal of the American Heart Association, 2020, 9, e017086.	3.7	7
33	Our work as health professionals: "With Great Power Comes Great Responsibility―[Stan Lee]. Journal of Nuclear Cardiology, 2020, 27, 1087-1088.	2.1	Ο
34	Selection of PET Camera and Implications on the Reliability and Accuracy of Absolute Myocardial Blood Flow Quantification. Current Cardiology Reports, 2020, 22, 109.	2.9	8
35	A Clinical Tool to Identify Candidates for Stress-First Myocardial Perfusion Imaging. JACC: Cardiovascular Imaging, 2020, 13, 2193-2202.	5.3	8
36	PET and SPECT Tracers for Myocardial Perfusion Imaging. Seminars in Nuclear Medicine, 2020, 50, 208-218.	4.6	39

#	Article	IF	CITATIONS
37	Test-Retest Precision of Myocardial Blood Flow Measurements With <sup>99m</sup> Tc-Tetrofosmin and Solid-State Detector Single Photon Emission Computed Tomography. Circulation: Cardiovascular Imaging, 2020, 13, e009769.	2.6	16
38	Reproducibility of cardiac magnetic resonance imaging in patients referred for the assessment of cardiac sarcoidosis; implications for clinical practice. International Journal of Cardiovascular Imaging, 2020, 36, 2199-2207.	1.5	4
39	Rubidium-82 generator yield and efficiency for PET perfusion imaging: Comparison of two clinical systems. Journal of Nuclear Cardiology, 2020, 27, 1728-1738.	2.1	11
40	Clinical comparison of the positron emission tracking (PeTrack) algorithm with the realâ€ŧime position management system for respiratory gating in cardiac positron emission tomography. Medical Physics, 2020, 47, 1713-1726.	3.0	8
41	Motion tracking of lowâ€activity fiducial markers using adaptive region of interest with listâ€mode positron emission tomography. Medical Physics, 2020, 47, 3402-3414.	3.0	3
42	The Future of Cardiac Molecular Imaging. Seminars in Nuclear Medicine, 2020, 50, 367-385.	4.6	19
43	Left atrial imaging and registration of fibrosis with conduction voltages using LGE-MRI and electroanatomical mapping. Computers in Biology and Medicine, 2019, 111, 103341.	7.0	5
44	Application of Hybrid Matrix Metalloproteinase-Targeted and Dynamic <sup>201</sup> Tl Single-Photon Emission Computed Tomography/Computed Tomography Imaging for Evaluation of Early Post-Myocardial Infarction Remodeling. Circulation: Cardiovascular Imaging, 2019, 12, e009055.	2.6	18
45	<sup>82</sup> Rb is the Best Flow Tracer for High-volume Sites. Annals of Nuclear Cardiology, 2019, 5, 53-62.	0.2	4
46	Patient body motion correction for dynamic cardiac <scp>PET</scp> â€ <scp>CT</scp> by attenuationâ€emission alignment according to projection consistency conditions. Medical Physics, 2019, 46, 1697-1706.	3.0	6
47	Phase analysis of gated PET in the evaluation of mechanical ventricular synchrony: A narrative overview. Journal of Nuclear Cardiology, 2019, 26, 1904-1913.	2.1	15
48	Whole-body motion correction in 13N-ammonia myocardial perfusion imaging using positron emission tracking. , 2019, , .		0
49	PET imaging of sympathetic innervation with [18F]Flurobenguan vs [11C]mHED in a patient with ischemic cardiomyopathy. Journal of Nuclear Cardiology, 2019, 26, 2151-2153.	2.1	10
50	SPECT quantification of myocardial blood flow: A journey of a thousand miles begins with a single step (Lao Tzu, Chinese philosopher, 604-531 BC). Journal of Nuclear Cardiology, 2019, 26, 772-774.	2.1	3
51	Saline-push improves rubidium-82 PET image quality. Journal of Nuclear Cardiology, 2019, 26, 1869-1874.	2.1	7
52	Prognostic utility of splenic response ratio in dipyridamole PET myocardial perfusion imaging. Journal of Nuclear Cardiology, 2019, 26, 1888-1897.	2.1	14
53	Clinical performance of Rb-82 myocardial perfusion PET and Tc-99m-based SPECT in patients with extreme obesity. Journal of Nuclear Cardiology, 2019, 26, 275-283.	2.1	16
54	Sensitivity and specificity of chest imaging for sarcoidosis screening in patients with cardiac presentations. Sarcoidosis Vasculitis and Diffuse Lung Diseases, 2019, 36, 18-24.	0.2	7

#	Article	IF	CITATIONS
55	Repeatable and reproducible measurements of myocardial oxidative metabolism, blood flow and external efficiency using 11C-acetate PET. Journal of Nuclear Cardiology, 2018, 25, 1912-1925.	2.1	13
56	Optimizing Risk Stratification and Noninvasive Diagnosis of Ischemic Heart Disease in Women. Canadian Journal of Cardiology, 2018, 34, 400-412.	1.7	7
57	Clinical Quantification of Myocardial Blood Flow Using PET: Joint Position Paper of the SNMMI Cardiovascular Council and the ASNC. Journal of Nuclear Cardiology, 2018, 25, 269-297.	2.1	151
58	PET Assessment of Epicardial Intimal Disease and Microvascular Dysfunction in Cardiac Allograft Vasculopathy. Journal of the American College of Cardiology, 2018, 71, 1444-1456.	2.8	71
59	Consistent tracer administration profile improves test–retest repeatability of myocardial blood flow quantification with 82Rb dynamic PET imaging. Journal of Nuclear Cardiology, 2018, 25, 929-941.	2.1	45
60	Effects of Hypercapnia on Myocardial Blood Flow in Healthy Human Subjects. Journal of Nuclear Medicine, 2018, 59, 100-106.	5.0	18
61	Lesion contrast recovery for partial-volume averaging: Quantitative correction or qualitative enhancement?. Journal of Nuclear Cardiology, 2018, 25, 1757-1759.	2.1	1
62	Clinical Quantification of Myocardial Blood Flow Using PET: Joint Position Paper of the SNMMI Cardiovascular Council and the ASNC. Journal of Nuclear Medicine, 2018, 59, 273-293.	5.0	163
63	Reporting myocardial flow reserve with PET. Ready or not, here it is! But walk before you fly!. Journal of Nuclear Cardiology, 2018, 25, 164-168.	2.1	5
64	False-positive 13N-ammonia positron emission tomography perfusion scan caused by misalignment of adjacent lung activity during attenuation correction. Journal of Nuclear Cardiology, 2018, 25, 1056-1058.	2.1	3
65	Whole-body motion correction in cardiac PET/CT using Positron Emission Tracking: A phantom validation study. , 2018, , .		2
66	Reproducible quantification of cardiac sympathetic innervation using graphical modeling of carbon-11-meta-hydroxyephedrine kinetics with dynamic PET-CT imaging. EJNMMI Research, 2018, 8, 63.	2.5	9
67	Effects of Riociguat on Right Ventricular Remodelling in Chronic Thromboembolic Pulmonary Hypertension Patients: A Prospective Study. Canadian Journal of Cardiology, 2018, 34, 1137-1144.	1.7	9
68	[18F]-Fluorodeoxyglucose PET/CT imaging as a marker of carotid plaque inflammation: Comparison to immunohistology and relationship to acuity of events. International Journal of Cardiology, 2018, 271, 378-386.	1.7	41
69	Coronary artery microvascular dysfunction: Role of sex and arterial load. International Journal of Cardiology, 2018, 270, 42-47.	1.7	18
70	Radionuclide Imaging in Decision-Making for Coronary Revascularization in Stable Ischemic Heart Disease. Current Cardiovascular Imaging Reports, 2018, 11, 1.	0.6	2
71	[ 18 F]-NaF PET/CT Identifies Active Calcification in Carotid Plaque. JACC: Cardiovascular Imaging, 2017, 10, 486-488.	5.3	38
72	Clinical PET Flow Reserve Imaging. JACC: Cardiovascular Imaging, 2017, 10, 578-581.	5.3	4

#	Article	IF	CITATIONS
73	Inter- and Intraobserver Agreement of <sup>18</sup> F-FDG PET/CT Image Interpretation in Patients Referred for Assessment of Cardiac Sarcoidosis. Journal of Nuclear Medicine, 2017, 58, 1324-1329.	5.0	32
74	Validation of a Multimodality Flow Phantom and Its Application for Assessment of Dynamic SPECT and PET Technologies. IEEE Transactions on Medical Imaging, 2017, 36, 132-141.	8.9	14
75	Radiation Safety in Children With Congenital and Acquired Heart Disease. JACC: Cardiovascular Imaging, 2017, 10, 797-818.	5.3	78
76	Optimization of SPECT Measurement of Myocardial Blood Flow with Corrections for Attenuation, Motion, and Blood Binding Compared with PET. Journal of Nuclear Medicine, 2017, 58, 2013-2019.	5.0	88
77	Evaluation of the clinical efficacy of the PeTrack motion tracking system for respiratory gating in cardiac PET imaging. Proceedings of SPIE, 2017, , .	0.8	3
78	N-Terminal Pro B-Type Natriuretic Peptide and High-Sensitivity Cardiac Troponin T Levels Are Related to the Extent of Hibernating Myocardium in Patients With Ischemic Heart Failure. Canadian Journal of Cardiology, 2017, 33, 1478-1488.	1.7	20
79	Time-frame sampling for 82Rb PET flow quantification: Towards standardization of clinical protocols. Journal of Nuclear Cardiology, 2017, 24, 1530-1534.	2.1	6
80	Status of cardiovascular PET radiation exposure and strategies for reduction: An Information Statement from the Cardiovascular PET Task Force. Journal of Nuclear Cardiology, 2017, 24, 1427-1439.	2.1	24
81	Characterization of 3-Dimensional PET Systems for Accurate Quantification of Myocardial Blood Flow. Journal of Nuclear Medicine, 2017, 58, 103-109.	5.0	61
82	False-positive stress PET–CT imaging in a patient with interstitial injection. Journal of Nuclear Cardiology, 2017, 24, 1447-1450.	2.1	8
83	Effects of an endothelin receptor antagonist, Macitentan, on right ventricular substrate utilization and function in a Sugen 5416/hypoxia rat model of severe pulmonary arterial hypertension. Journal of Nuclear Cardiology, 2017, 24, 1979-1989.	2.1	23
84	Optimally Repeatable Kinetic Model Variant for Myocardial Blood Flow Measurements with <sup>82</sup> Rb PET. Computational and Mathematical Methods in Medicine, 2017, 2017, 1-11.	1.3	8
85	Dual Spillover Correction for SPECT Myocardial Blood Flow Measurement. , 2017, , .		Ο
86	Reply: Variation in Maximum Counting Rates During Myocardial Blood Flow Quantification Using <sup>82</sup> Rb PET. Journal of Nuclear Medicine, 2017, 58, 519-520.	5.0	3
87	Cardiac PET Imaging: Principles and New Developments. , 2017, , 451-483.		1
88	Randomized Trial Comparing the Effects of Ticagrelor Versus Clopidogrel on Myocardial Perfusion in Patients With Coronary Artery Disease. Journal of the American Heart Association, 2017, 6, .	3.7	10
89	Patient motion effects on the quantification of regional myocardial blood flow with dynamic PET imaging. Medical Physics, 2016, 43, 1829-1840.	3.0	68
90	Women Image Wisely. JACC: Cardiovascular Imaging, 2016, 9, 385-387.	5.3	7

#	Article	IF	CITATIONS
91	Long-Term Follow-Up of Outcomes With F-18-Fluorodeoxyglucose Positron Emission Tomography Imaging–Assisted Management of Patients With Severe Left Ventricular Dysfunction Secondary to Coronary Disease. Circulation: Cardiovascular Imaging, 2016, 9, .	2.6	60
92	Reduced Myocardial Flow in Heart Failure Patients With Preserved Ejection Fraction. Circulation: Heart Failure, 2016, 9, .	3.9	99
93	PET Metabolic Biomarkers for Cancer. Biomarkers in Cancer, 2016, 8s2, BIC.S27483.	3.6	17
94	82Rb PET imaging of myocardial blood flow—have we achieved the 4 "Râ€s to support routine use?. EJNMMI Research, 2016, 6, 69.	2.5	6
95	Decreased renal AT1 receptor binding in rats after subtotal nephrectomy: PET study with [18F]FPyKYNE-losartan. EJNMMI Research, 2016, 6, 55.	2.5	4
96	Clinical PET Myocardial Perfusion Imaging and Flow Quantification. Cardiology Clinics, 2016, 34, 69-85.	2.2	34
97	Radionuclide Tracers for Myocardial Perfusion Imaging and Blood Flow Quantification. Cardiology Clinics, 2016, 34, 37-46.	2.2	15
98	Respiratory motion resulting in a pseudo-ischemia pattern on stress PET–CT imaging. Journal of Nuclear Cardiology, 2016, 23, 159-160.	2.1	6
99	Myocardial blood flow quantification by Rb-82 cardiac PET/CT: A detailed reproducibility study between two semi-automatic analysis programs. Journal of Nuclear Cardiology, 2016, 23, 499-510.	2.1	29
100	Shifts in myocardial fatty acid and glucose metabolism in pulmonary arterial hypertension: a potential mechanism for a maladaptive right ventricular response. European Heart Journal Cardiovascular Imaging, 2016, 17, 1424-1431.	1.2	53
101	Noninvasive PET Flow Reserve Imaging to Direct Optimal Therapies for Myocardial Ischemia. , 2016, , 153-170.		0
102	Sci-Fri AM: MRI and Diagnostic Imaging - 05: Comparison of Input Function Measurements from DCE and MOLLI. Medical Physics, 2016, 43, 4952-4952.	3.0	0
103	Development of reporter gene imaging techniques for long-term assessment of human circulating angiogenic cells. Biomedical Materials (Bristol), 2015, 10, 034104.	3.3	1
104	Single low-dose CT scan optimized for rest-stress PET attenuation correction and quantification of coronary artery calcium. Journal of Nuclear Cardiology, 2015, 22, 419-428.	2.1	27
105	PET imaging of a collagen matrix reveals its effective injection and targeted retention in a mouse model of myocardial infarction. Biomaterials, 2015, 49, 18-26.	11.4	20
106	Biodistribution and radiation dosimetry of 82Rb at rest and during peak pharmacological stress in patients referred for myocardial perfusion imaging. European Journal of Nuclear Medicine and Molecular Imaging, 2015, 42, 1032-1042.	6.4	37
107	Test–retest repeatability of myocardial blood flow and infarct size using 11C-acetate micro-PET imaging in mice. European Journal of Nuclear Medicine and Molecular Imaging, 2015, 42, 1589-1600.	6.4	8
108	Reduced dose measurement of absolute myocardial blood flow using dynamic SPECT imaging in a porcine model. Medical Physics, 2015, 42, 5075-5083.	3.0	9

#	Article	IF	CITATIONS
109	β2-adrenergic stress evaluation of coronary endothelial-dependent vasodilator function in mice using 11C-acetate micro-PET imaging of myocardial blood flow and oxidative metabolism. EJNMMI Research, 2014, 4, 68.	2.5	6
110	Quantification of myocardial blood flow using PET to improve the management of patients with stable ischemic coronary artery disease. Future Cardiology, 2014, 10, 611-631.	1.2	13
111	Prevalence of Cardiac Sarcoidosis in Patients Presenting with Monomorphic Ventricular Tachycardia. PACE - Pacing and Clinical Electrophysiology, 2014, 37, 364-374.	1.2	96
112	Detection and severity classification of extracardiac interference in <sup>82</sup> Rb PET myocardial perfusion imaging. Medical Physics, 2014, 41, 102501.	3.0	7
113	Dynamic SPECT Measurement of Absolute Myocardial Blood Flow in a Porcine Model. Journal of Nuclear Medicine, 2014, 55, 1685-1691.	5.0	134
114	Effects of Short-Term Continuous Positive Airway Pressure on Myocardial Sympathetic Nerve Function and Energetics in Patients With Heart Failure and Obstructive Sleep Apnea. Circulation, 2014, 130, 892-901.	1.6	80
115	Absolute myocardial flow quantification with 82Rb PET/CT: comparison of different software packages and methods. European Journal of Nuclear Medicine and Molecular Imaging, 2014, 41, 126-135.	6.4	77
116	SPECT gated blood pool phase analysis of lateral wall motion for prediction of CRT response. International Journal of Cardiovascular Imaging, 2014, 30, 559-569.	1.5	10
117	Regional Myocardial Sympathetic Denervation Predicts the Risk of Sudden Cardiac Arrest in Ischemic Cardiomyopathy. Journal of the American College of Cardiology, 2014, 63, 141-149.	2.8	351
118	Quantification of Myocardial Blood Flow inÂAbsolute Terms Using 82Rb PET Imaging. JACC: Cardiovascular Imaging, 2014, 7, 1119-1127.	5.3	144
119	Feasibility and operator variability of myocardial blood flow and reserve measurements with 99mTc-sestamibi quantitative dynamic SPECT/CT imaging. Journal of Nuclear Cardiology, 2014, 21, 1075-1088.	2.1	54
120	Clinical Interpretation Standards and Quality Assurance for the Multicenter PET/CT Trial Rubidium-ARMI. Journal of Nuclear Medicine, 2014, 55, 58-64.	5.0	40
121	Prognostic Value of Rubidium-82 Positron Emission Tomography in Patients After Heart Transplant. Circulation: Cardiovascular Imaging, 2014, 7, 930-937.	2.6	96
122	Early diabetes treatment does not prevent sympathetic dysinnervation in the streptozotocin diabetic rat heart. Journal of Nuclear Cardiology, 2014, 21, 829-841.	2.1	10
123	The role of integrin α2 in cell and matrix therapy that improves perfusion, viability and function of infarcted myocardium. Biomaterials, 2014, 35, 4749-4758.	11.4	34
124	Patient-Centered Imaging. Journal of the American College of Cardiology, 2014, 63, 1480-1489.	2.8	122
125	List-mode motion tracking for positron emission tomography imaging using low-activity fiducial markers. , 2014, , .		1
126	Cardiac Micro-PET-CT. Current Cardiovascular Imaging Reports, 2013, 6, 179-190.	0.6	0

#	Article	IF	CITATIONS
127	Insulin restores myocardial presynaptic sympathetic neuronal integrity in insulin-resistant diabetic rats. Journal of Nuclear Cardiology, 2013, 20, 845-856.	2.1	16
128	Characterizing the normal range of myocardial blood flow with 82rubidium and 13N-ammonia PET imaging. Journal of Nuclear Cardiology, 2013, 20, 578-591.	2.1	54
129	Alternative Imaging Modalities in Ischemic Heart Failure (AIMI-HF) IMAGE HF Project I-A: study protocol for a randomized controlled trial. Trials, 2013, 14, 218.	1.6	51
130	Test–retest repeatability of quantitative cardiac 11C-meta-hydroxyephedrine measurements in rats by small animal positron emission tomography. Nuclear Medicine and Biology, 2013, 40, 676-681.	0.6	28
131	Cardiac PET: Metabolic and Functional Imaging of the Myocardium. Seminars in Nuclear Medicine, 2013, 43, 434-448.	4.6	31
132	Multisoftware Reproducibility Study of Stress and Rest Myocardial Blood Flow Assessed with 3D Dynamic PET/CT and a 1-Tissue-Compartment Model of <sup>82</sup> Rb Kinetics. Journal of Nuclear Medicine, 2013, 54, 571-577.	5.0	110
133	Preclinical Evaluation of Biopolymer-Delivered Circulating Angiogenic Cells in a Swine Model of Hibernating Myocardium. Circulation: Cardiovascular Imaging, 2013, 6, 982-991.	2.6	10
134	Repeatable Noninvasive Measurement of Mouse Myocardial Glucose Uptake with <sup>18</sup> F-FDG: Evaluation of Tracer Kinetics in a Type 1 Diabetes Model. Journal of Nuclear Medicine, 2013, 54, 1637-1644.	5.0	35
135	Current and Future Clinical Applications of Cardiac Positron Emission Tomography. Circulation Journal, 2013, 77, 836-848.	1.6	25
136	Respiratory phase alignment improves blood-flow quantification in Rb82 PET myocardial perfusion imaging. Medical Physics, 2013, 40, 022503.	3.0	16
137	PET Radiopharmaceuticals. , 2013, , 115-125.		0
138	Measuring coronary artery calcification using positron emission tomography-computed tomography attenuation correction images. European Heart Journal Cardiovascular Imaging, 2012, 13, 786-792.	1.2	43
139	A three-dimensional model-based partial volume correction strategy for gated cardiac mouse PET imaging. Physics in Medicine and Biology, 2012, 57, 4309-4334.	3.0	7
140	<sup>18</sup> F-FDG Cell Labeling May Underestimate Transplanted Cell Homing: More Accurate, Efficient, and Stable Cell Labeling with Hexadecyl-4-[ <sup>18</sup> F]Fluorobenzoate for in Vivo Tracking of Transplanted Human Progenitor Cells by Positron Emission Tomography. Cell Transplantation, 2012, 21, 1821-1835.	2.5	29
141	Uniformity and repeatability of normal resting myocardial blood flow in rats using [13N]-ammonia and small animal PET. Nuclear Medicine Communications, 2012, 33, 917-925.	1.1	11
142	Does Rubidium-82 PET Have Superior Accuracy to SPECT Perfusion Imaging for the Diagnosis of Obstructive Coronary Disease?. Journal of the American College of Cardiology, 2012, 60, 1828-1837.	2.8	297
143	Short-term repeatability of resting myocardial blood flow measurements using rubidium-82 PET imaging. Journal of Nuclear Cardiology, 2012, 19, 997-1006.	2.1	68
144	Accuracy of low-dose rubidium-82 myocardial perfusion imaging for detection of coronary artery disease using 3D PET and normal database interpretation. Journal of Nuclear Cardiology, 2012, 19, 1135-1145.	2.1	40

#	Article	IF	CITATIONS
145	Imaging atherosclerosis with hybrid [18F]fluorodeoxyglucose positron emission tomography/computed tomography imaging: What Leonardo da Vinci could not see. Journal of Nuclear Cardiology, 2012, 19, 1211-1225.	2.1	55
146	Analysis of (R)- and (S)-[11C]rolipram Kinetics in Canine Myocardium for the Evaluation of Phosphodiesterase-4 with PET. Molecular Imaging and Biology, 2012, 14, 225-236.	2.6	9
147	Does quantification of myocardial flow reserve using rubidium-82 positron emission tomography facilitate detection of multivessel coronary artery disease?. Journal of Nuclear Cardiology, 2012, 19, 670-680.	2.1	252
148	Quantification of regional myocardial blood flow estimation with three-dimensional dynamic rubidium-82 PET and modified spillover correction model. Journal of Nuclear Cardiology, 2012, 19, 763-774.	2.1	31
149	Impaired Myocardial Flow Reserve on Rubidium-82 Positron Emission Tomography Imaging Predicts Adverse Outcomes in Patients Assessed for Myocardial Ischemia. Journal of the American College of Cardiology, 2011, 58, 740-748.	2.8	498
150	Incremental Diagnostic Value of Regional Myocardial Blood Flow Quantification Over Relative Perfusion Imaging With Generator-Produced Rubidium-82 PET. Circulation Journal, 2011, 75, 2628-2634.	1.6	50
151	Incremental prognostic value of coronary flow reserve assessed with single-photon emission computed tomography. Journal of Nuclear Cardiology, 2011, 18, 541-543.	2.1	2
152	Relation Between Right Ventricular Function and Increased Right Ventricular [ <sup>18</sup> F]Fluorodeoxyglucose Accumulation in Patients With Heart Failure. Circulation: Cardiovascular Imaging, 2011, 4, 59-66.	2.6	63
153	PET of ( <i>R</i> )- <sup>11</sup> C-Rolipram Binding to Phosphodiesterase-4 Is Reproducible and Sensitive to Increased Norepinephrine in the Rat Heart. Journal of Nuclear Medicine, 2011, 52, 263-269.	5.0	16
154	Kinetic modelâ€based factor analysis of dynamic sequences for 82â€rubidium cardiac positron emission tomography. Medical Physics, 2010, 37, 3995-4010.	3.0	18
155	Quantitative analysis of coronary endothelial function with generator-produced 82Rb PET: comparison with 150-labelled water PET. European Journal of Nuclear Medicine and Molecular Imaging, 2010, 37, 2233-2241.	6.4	35
156	Intra- and inter-operator repeatability of myocardial blood flow and myocardial flow reserve measurements using rubidium-82 pet and a highly automated analysis program. Journal of Nuclear Cardiology, 2010, 17, 600-616.	2.1	126
157	An abbreviated hyperinsulinemic-euglycemic clamp results in similar myocardial glucose utilization in both diabetic and non-diabetic patients with ischemic cardiomyopathy. Journal of Nuclear Cardiology, 2010, 17, 637-645.	2.1	18
158	SPECT blood pool phase analysis can accurately and reproducibly quantify mechanical dyssynchrony. Journal of Nuclear Cardiology, 2010, 17, 803-810.	2.1	13
159	Quantification of myocardial blood flow and flow reserve: Technical aspects. Journal of Nuclear Cardiology, 2010, 17, 555-570.	2.1	149
160	3D versus 2D dynamic 82Rb myocardial blood flow imaging in a canine model of stunned and infarcted myocardium. Nuclear Medicine Communications, 2010, 31, 75-81.	1.1	7
161	Quantification of regional myocardial blood flow in a canine model of stunned and infarcted myocardium: comparison of rubidium-82 positron emission tomography with microspheres. Nuclear Medicine Communications, 2010, 31, 67-74.	1.1	11
162	Diagnosis and Prognosis in Cardiac Disease Using Cardiac PET Perfusion Imaging. , 2010, , 309-331.		4

#	Article	IF	CITATIONS
163	Quantification of Myocardial Blood Flow Using Rubidium-82 PET. , 2010, , 78-90.		0
164	Repeatability of Rest and Hyperemic Myocardial Blood Flow Measurements with <sup>82</sup> Rb Dynamic PET. Journal of Nuclear Medicine, 2009, 50, 68-71.	5.0	92
165	Quantification of myocardial perfusion: What will it take to make it to prime time?. Current Cardiovascular Imaging Reports, 2009, 2, 238-249.	0.6	2
166	3D list-mode cardiac PET for simultaneous quantification of myocardial blood flow and ventricular function. , 2008, , .		6
167	Respiratory-motion errors in quantitative myocardial perfusion with PET/CT. , 2007, , .		2
168	The Effects of Continuous Positive Airway Pressure on Myocardial Energetics in Patients With Heart Failure and Obstructive Sleep Apnea. Journal of the American College of Cardiology, 2007, 49, 450-458.	2.8	66
169	F-18-Fluorodeoxyglucose Positron Emission Tomography Imaging-Assisted Management of Patients With Severe Left Ventricular Dysfunction and Suspected Coronary Disease. Journal of the American College of Cardiology, 2007, 50, 2002-2012.	2.8	403
170	Will 3-dimensional PET-CT enable the routine quantification of myocardial blood flow?. Journal of Nuclear Cardiology, 2007, 14, 380-397.	2.1	86
171	Quantification of myocardial blood flow with 82Rb dynamic PET imaging. European Journal of Nuclear Medicine and Molecular Imaging, 2007, 34, 1765-1774.	6.4	373
172	Coronary x-ray angiographic reconstruction and image orientation. Medical Physics, 2006, 33, 707-718.	3.0	18
173	Constant-Activity-Rate Infusions for Myocardial Blood Flow Quantification with 82Rb and 3D PET. , 2006, , .		4
174	What is the Prognostic Value of Myocardial Perfusion Imaging Using Rubidium-82 Positron Emission Tomography?. Journal of the American College of Cardiology, 2006, 48, 1029-1039.	2.8	333
175	Prediction of Arrhythmic Events with Positron Emission Tomography: PAREPET study design and methods. Contemporary Clinical Trials, 2006, 27, 374-388.	1.8	53
176	Application of Cardiac Molecular Imaging Using Positron Emission Tomography in Evaluation of Drug and Therapeutics for Cardiovascular Disorders. Current Pharmaceutical Design, 2005, 11, 903-932.	1.9	46
177	Regional 11C-hydroxyephedrine retention in hibernating myocardium: chronic inhomogeneity of sympathetic innervation in the absence of infarction. Journal of Nuclear Medicine, 2005, 46, 1368-74.	5.0	65
178	A infusion system for quantitative perfusion imaging with 3D PET. Applied Radiation and Isotopes, 2004, 60, 921-927.	1.5	13
179	Evaluation of outcome and cost-effectiveness using an FDG PET-guided approach to management of patients with coronary disease and severe left ventricular dysfunction (PARR-2): rationale, design, and methods. Contemporary Clinical Trials, 2003, 24, 776-794.	1.9	22
180	Positron emission tomography and recovery following revascularization (PARR-1): the importance of scar and the development of a prediction rule for the degree of recovery of left ventricular function. Journal of the American College of Cardiology, 2002, 40, 1735-1743.	2.8	174

#	Article	IF	CITATIONS
181	Manufacture of strontium-82/rubidium-82 generators and quality control of rubidium-82 chloride for myocardial perfusion imaging in patients using positron emission tomography. Applied Radiation and Isotopes, 1999, 50, 1015-1023.	1.5	36
182	Automated determination of the left ventricular long axis in cardiac positron tomography. Physiological Measurement, 1996, 17, 95-108.	2.1	29